Catalystlike behavior of Si adatoms in the growth of monolayer Al film on Si(111)

Jing Teng, Lixin Zhang, Ying Jiang, Jiandong Guo, Qinlin Guo, Enge Wang, Philipp Ebert, T. Sakurai, and Kehui Wu

Citation: The Journal of Chemical Physics **133**, 014704 (2010); doi: 10.1063/1.3455231
View online: http://dx.doi.org/10.1063/1.3455231
View Table of Contents: http://scitation.aip.org/content/aip/journal/jcp/133/1?ver=pdfcov
Published by the AIP Publishing

Catalystlike behavior of Si adatoms in the growth of monolayer Al film on Si(111)

Jing Teng,[1] Lixin Zhang,[2] Ying Jiang,[1] Jiandong Guo,[1] Qinlin Guo,[1] Enge Wang,[1] Philipp Ebert,[3] T. Sakurai,[4] and Kehui Wu[1,a)]
[1]*Institute of Physics, Chinese Academy of Sciences, Beijing 100080, China*
[2]*National Renewable Energy Laboratory, Golden, Colorado 80401, USA*
[3]*Institut für Festkörperforschung, Forschungszentrum Jülich GmbH, 52425 Jülich, Germany*
[4]*Institute for Materials Research, Tohoku University, Sendai 980-8577, Japan*

(Received 2 February 2010; accepted 27 May 2010; published online 7 July 2010)

The formation mechanism of monolayer Al(111)1×1 film on the Si(111)$\sqrt{3}\times\sqrt{3}$-Al substrate was studied by scanning tunneling microscopy and first-principles calculations. We found that the Si adatoms on the $\sqrt{3}\times\sqrt{3}$-Al substrate play important roles in the growth process. The growth of Al-1×1 islands is mediated by the formation and decomposition of $SiAl_2$ clusters. Based on experiments and theoretical simulations we propose a model where free Si atoms exhibit a catalystlike behavior by capturing and releasing Al atoms during the Al film growth.
 [doi:10.1063/1.3455231]

I. INTRODUCTION

Epitaxial growth in ultrahigh vacuum (UHV) is a nonequilibrium process where the competition between kinetics and energetics results in rich surface growth phenomena, which are attracting persistent interest as they provide opportunities of manufacturing various metastable, low-dimensional, and nanostructures.[1,2] For example, atomically smooth and ultrathin metal films, which exhibit unique physical and chemical properties due to the quantization of free electrons in the vertical direction,[3–7] may be obtained by using low temperature deposition to freeze the diffusion of metal atoms.[8–10] In contrast, growth at room temperature usually results in the formation of three-dimensional (3D) islands. Moreover, in the case of metal films on semiconductor surfaces, due to the high interface energy, there usually exists a critical thickness, typically 4–6 monolayer (ML), below which a continuous film cannot be formed even with the low-temperature deposition.[11–15] In a recent work, Jiang *et al.*[16] reported the growth of atomically smooth Al(111) films on Si(111), with continuously controllable thickness down to the extreme level of 1 ML, which provides an ideal two-dimensional (2D) system for exploring the thickness dependent effects in jellium metals. Interestingly, the growth could be performed at room temperature, indicating that the growth kinetics in their method is quite different from conventional low temperature growth of metal films. Further study is therefore desired to understand the mechanism therein, especially with the 1 ML Al(111) film.

In this paper we report on the observation of an unexpected Si adatom-mediated mechanism in the growth of 1 ML Al(111)1×1 film on Si(111). The Si adatoms in the initial Si(111)$\sqrt{3}\times\sqrt{3}$-Al surface act as seeds to form $SiAl_2$ clusters. The clusters are then transformed into Al(111)1×1 via the incorporation of further incoming Al atoms, and spontaneously releasing the Si atoms which may participate in the next cycle of the clustering process. The Si adatoms serve as a surface active agent, in analogy to a catalyst. As a result, a 2D growth of monolayer Al(111) is achieved.

II. EXPERIMENTS

Experiments were performed in a dual-chamber UHV system equipped with a scanning tunneling microscope (STM) and a low energy electron diffraction (LEED) optics, the base pressure being 5×10^{-11} Torr. The substrate was cut from a *n*-type Si(111) wafer (phosphor-doped, resistivity of ~2 Ω cm). A clean Si(111) surface was prepared by standard flashing to 1550 K. The $\sqrt{3}\times\sqrt{3}$-Al surface was prepared by depositing ~0.19 ML Al atoms [1 ML refers to the atomic density of the Al(111) plane in this paper, 0.19 ML here corresponds to 1/3 ML with respect to the atomic density of the Si(111) plane] to a clean Si(111)7×7 surface, followed by annealing to 1000 K for 2 min. The resulting $\sqrt{3}\times\sqrt{3}$-Al surface was used as the substrate for subsequent growth of Al films at room temperature. After preparation, the sample was transferred *in situ* to the analysis chamber for STM and LEED investigations. All STM images were recorded in constant current (60 pA) mode with a chemically etched tungsten tip.

III. RESULTS AND DISCUSSIONS

The Si(111)$\sqrt{3}\times\sqrt{3}$-Al surface consists of Al adatoms on the T4 sites of a bulk-truncated Si(111)1×1. Each Al adatom is bonded to three second-layer Si atoms.[17] Typical filled state STM images of a clean $\sqrt{3}\times\sqrt{3}$-Al surface are shown in Figs. 1(a) and 1(f). Another well-known feature of the $\sqrt{3}\times\sqrt{3}$-Al surface is that some of the Al adatom sites are occupied by Si atoms. These sites are imaged as randomly distributed bright protrusions in filled state STM images, e.g., the brighter atoms in Fig. 1(a).[17,18] Interestingly, the

a)Author to whom correspondence should be addressed. Electronic mail: khwu@aphy.iphy.ac.cn.

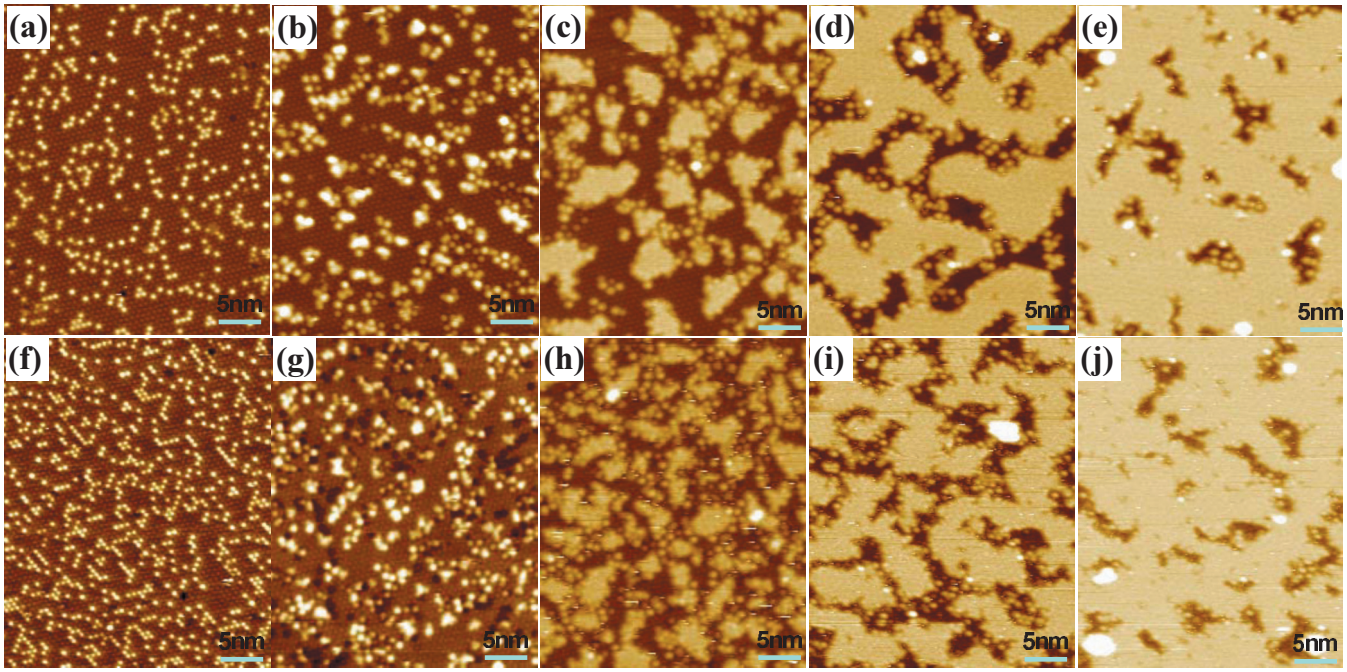

FIG. 1. [(a) and (f)] Filled state STM images of two $\sqrt{3}\times\sqrt{3}$-Al surfaces with different Si adatom densities, 0.026 and 0.043 ML, respectively. Note that the darker, close-pack protrusions are $\sqrt{3}\times\sqrt{3}$-Al adatoms. [(b)–(e) and (g)–(j)] The morphology evolution of Al grown on the two $\sqrt{3}\times\sqrt{3}$-Al substrates with increasing Al coverage. The total Al coverages are (a) 0.16, (b) 0.25, (c) 0.43, (d) 0.71, (e) 0.89, (f) 0.14, (g) 0.24, (h) 0.43, (i) 0.72, and (j) 0.91 ML. All images were taken at sample bias of −2.0 V.

density of these substitutional Si adatoms can be tuned by adjusting the amount of Al atoms deposited in the preparation of $\sqrt{3}\times\sqrt{3}$-Al surface. Because the total coverage of Al adatoms and Si adatoms is 0.19 ML [1/3 of the atomic density of the Si(111) plane], higher Al coverage will result in lower Si adatom density. Figures 1(a) and 1(f) are two $\sqrt{3}\times\sqrt{3}$-Al surfaces with different initial Si adatom densities, 0.026 and 0.043 ML, respectively.

The growth process of Al on the $\sqrt{3}\times\sqrt{3}$-Al surface is illustrated in Figs. 1(b)–1(e) and 1(g)–1(j) for two series of samples with different initial Si adatom densities as mentioned above. Small clusters and nuclei are formed [(b) and (g)] initially, followed by the formation of monolayer Al islands [(c) and (h)]. With increasing Al coverage, the Al islands grow two-dimensionally until they percolate to form a continuous film. Eventually a complete and atomically smooth monolayer Al film is obtained. Furthermore, comparing the two series of samples, we found that the densities of the nucleation sites and Al islands are obviously higher in the sample with higher Si adatom density. Therefore, the Si adatoms should play a role of promoting the nucleation of Al islands.

In addition, we notice another main feature in these STM images: the emergence of many identical, round-shape protrusions surrounding the Al islands. These protrusions, or clusters, are particularly abundant in the middle Al coverage range, as shown in Figs. 1(b)–1(d) and 1(g)–1(i), while they vanish as the film growth completes. Figure 2 shows a closer view of the clusters in filled and empty state STM images. The clusters prefer to locate around the edge of the Al-1 $\times$1 islands, and some form local 2$\times$2 domains with respect to the Si(111) substrate [white arrows in Fig. 2(a)]. The clusters have a distinguishable electronic structure compared with that of Al-1$\times$1 islands. In the filled-state image it is about the same height as the Al-1$\times$1 islands, while in the empty-state images it appears as a dark feature. In the dI/dV spectra it shows a significant larger bandgap compared with that of the nearly metallic Al-1$\times$1 islands [Fig. 2(c)]. These Al clusters, including both those at the edge of Al islands and those arranged into 2$\times$2 pads, are energetically quite stable. They do not automatically merge or transform into Al-1 $\times$1 after prolonged scanning (>10 h) or even applying voltage pulse (± 5 V) above the clusters. The cluster is an intermediate structure, as it will eventually be converted to Al-1$\times$1 upon the completion of the Al-1$\times$1 film.

A quantitative analysis of the total area of the Al-1$\times$1 islands ($Al_{1\times1}$), the number of Al clusters (N_c), and the number of Si adatoms as a function of the total coverage of Al (including the initial $\sqrt{3}\times\sqrt{3}$-Al adatoms and subsequently deposited Al atoms) is shown in Fig. 3 for the two series of samples shown in Fig. 1. The number of Al clusters increases with the increasing Al coverage initially, reaching a maximum at certain Al coverage, and finally diminishes to zero at 1 ML. From this analysis we are able to derive the exact number of Al atoms contained in each Al cluster. Because Al atoms exist in three forms, the Al-1$\times$1 islands, the remaining $\sqrt{3}\times\sqrt{3}$-Al adatoms, and the Al clusters, we have

$$N_{Al} = N_{root3} + Al_{1\times1} \times \theta_{1\times1} + N_c \times n.$$

Here N_{Al} is the total amount of Al atoms on the surface, which is known through our flux calibration; N_{root3} is the number of remaining $\sqrt{3}\times\sqrt{3}$-Al adatoms, which can be counted in the atomically resolved STM images; $\theta_{1\times1}$ is the density of Al atoms in Al-1$\times$1 film, 13.9 nm^{-2}; $Al_{1\times1}$ is the measured area ratio of Al islands; and n is the number of Al atoms in each cluster. In writing the above equation one

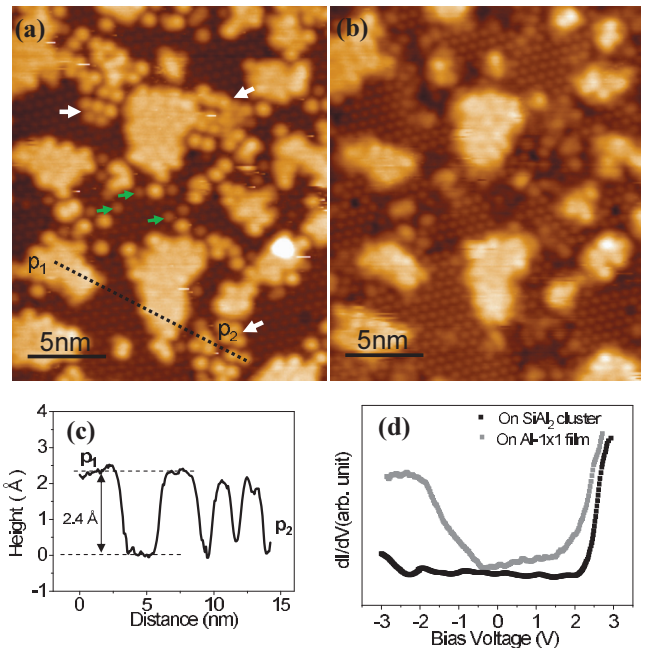

FIG. 2. [(a) and (b)] Atomically resolved STM images of the $SiAl_2$ clusters in the filled-state (−2.0 V) and empty-state (2.0 V), respectively. The brightest, rounded protrusions are $SiAl_2$ clusters, and some less-bright protrusions, as indicated by green arrows in the center part of the image, are remaining Si adatoms. The close-pack protrusions in the background are $\sqrt{3}\times\sqrt{3}$-Al adatoms. Local 2×2 patches of $SiAl_2$ clusters can be observed, as marked by the white arrows. (c) The height profile as marked in (a) showing the Al-1×1 islands (2.4 Å) and $SiAl_2$ clusters of about the same height. (d) dI/dV spectra taken on the Al-1×1 island and on the $SiAl_2$ cluster, respectively. The latter one shows a larger bandgap.

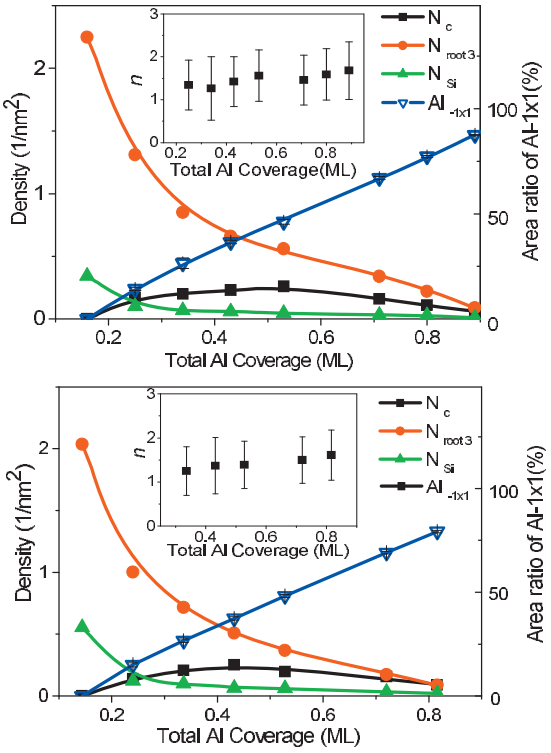

FIG. 3. [(a) and (b)] The statistical results of $Al_{1\times1}$ (total area ratio of Al-1×1 islands in blue curve), N_c (number of Al clusters in black curve), $N_{Al\text{-}\sqrt{3}}$ (number of $\sqrt{3}\times\sqrt{3}$-Al adatoms in red curve), and N_{Si} (number of Si adatoms in green curve) as a function of the total Al coverage for the two series of samples with initial Si adatom density of 0.026 and 0.043 ML, respectively. Note that the X axis is the total Al coverage, including Al atoms in all forms. The insets are the calculated n representing the number of Al atoms in each cluster.

should note that there is no $\sqrt{3}\times\sqrt{3}$-Al structure underneath the Al-1×1 islands, i.e., the Al-1×1 film is formed directly on Si(111)-1×1. (The initial $\sqrt{3}\times\sqrt{3}$-Al adatoms are spontaneously incorporated into the Al-1×1 film during growth.)[16] Here n is the only variable, as all other parameters can be calculated from the STM image (N_{root3}, $Al_{1\times1}$, N_c) or are known parameters (N_{Al}, $\theta_{1\times1}$).

We calculated n for various samples with different initial Si adatom densities and Al coverages, as shown in the insets of Figs. 3(a) and 3(b). For 12 data points we obtained a constant value of about 1.6, i.e., most likely two Al atoms in a cluster. We should note that based on STM images, experimentally measured area of islands is always systematically larger than the real value. This is because the STM tip has a certain radius, resulting in the position of the step edge of islands always outside its real position. Note that the area of Al islands relies on where we set the edge of the Al islands. In this work we make three choices of the step edges: inner, middle, and outer edges. The difference between the inner and outer edges gives the error bar for the area determination. One can see that if we chose the inner edge, which is more close to the real situation, the resulted n is very close to 2. Therefore we believe $n=2$ is quantitatively consistent with our experiment. In addition, the increase of the number of clusters is accomplished by the decrease of the number of Si adatoms. Therefore, it is very likely that each magic cluster consists of one Si atom that can be regarded as the "core" of a cluster.

The above observations suggest that the Si adatoms assist the nucleation and growth of Al-1×1 islands, not simply as surface defect sites that may enhance nucleation,[19,20] but rather through the formation of an intermediate $SiAl_2$ cluster state that bridges the free Al atoms and the Al-1×1 phase. Upon the formation, the Si adatom will be released again and may participate in the next clustering-releasing cycle. This in some sense is similar to a catalyst-promoted chemical reaction process where the Si adatom is the catalyst.

IV. THEORETICAL SIMULATIONS

To confirm this assumption, we performed extensive first-principles calculations based on the density functional theory and the VASP code.[21] We used the projector-augmented wave method with generalized gradient approximation (GGA) potentials.[22] The Si(111) surface is modeled by a supercell of 2×2 or 3×3 in x-y plane. Along z-axis, the simulation slab includes five bilayers of Si, and a vacuum of ~14 Å, of which the bottom Si layer is fixed and passivated by hydrogen atoms. The cutoff energy used for the plane-wave basis set is 250 eV, and the k-points sampling in the Brillouin zone is done with a $4\times4\times1$ mesh. The calculated equilibrium lattice constants for Si and Al are 5.47 and 4.05 Å (experiments: 5.43 and 4.05 Å). In order to compare the energetics of different structures, the formation energies are calculated using

$$E_f = E_{\text{tot}} - (E_s + n_{\text{Si}} \cdot \mu_{\text{Si}} + n_{\text{Al}} \cdot \mu_{\text{Al}}),$$

where E_{tot} is the total energy of the structure; E_s is the total energy of the reference structure, i.e., an ideal $\sqrt{3}\times\sqrt{3}$-Al surface; n_{Si} (n_{Al}) is the number of added Si (Al) atoms from a bulk reservoir to the reference structure in order to form the structure; and μ_{Si} (μ_{Al}) is the chemical potential of the reservoir. In this study, the chemical potentials are chosen as the respective bulk values, so they do not present as variables in the calculated formation energies.

In the first step we investigate the adsorption of one Al atom on the $\sqrt{3}\times\sqrt{3}$-Al surface. To represent a real surface, 1/3 of the Al adatoms were replaced by Si adatoms on a 3×3 surface which include three $\sqrt{3}\times\sqrt{3}$ units. Both Al and Si adatoms prefer to occupy the T4 sites on the Si(111) surface. The Al adatom is 0.6 eV more favorable than the Si adatom in formation energy. Therefore, with floating Al atoms around the Si adatom, the Si adatom bonds can be easily broken by the insertion of the Al atom, which lowers the surface energy. Note that this does not contradict with the fact that a $\sqrt{3}\times\sqrt{3}$-Al surface always contains Si adatoms, which is an entropy effect that was not accounted for in our calculation.

To understand the structure of the "magic clusters," we have explored various structure models consisting of different number of Al atoms around a Si adatom. As discussed above, a deposited Al atom will automatically locate and replace a Si adatom, but the replaced Si adatom does not go away. Instead, it forms a SiAl cluster with a further incoming Al atom, the formation energy being 0.6 eV by our calculation. We should note that although the formation energy is positive, the surface energy is lowered with the formation of SiAl cluster. For the further incoming Al atoms, the most favorable site is the existing SiAl cluster to form the $SiAl_2$ cluster, with the formation energy of 0.4 eV. At this point, to incorporate more Al atoms into the $SiAl_2$ cluster is the least preferred process with formation energy of 2.15 eV. As a result, most SiAl clusters will be transformed to $SiAl_2$. This is in good agreement with our experimental estimation that each cluster contains two Al atoms and one Si atom. Some SiAl clusters may coexist with the SiAl2 clusters, but the amount should be negligible except at the very initial stage of growth where the amount of Al atoms is insufficient to convert all the clusters to SiAl2.

We should note that the formation energy depends on the reference structure. If we choose the Si(111)7×7 surface as the reference structure, the formation energies of the SiAl and $SiAl_2$ are all negative, thus they are stable. The structure model of a $SiAl_2$ cluster, around the T4 site, is illustrated in Figs. 4(a) and 4(b). For such an isolated cluster, the simulated STM image shows that the center of the cluster is not located exactly at the $\sqrt{3}\times\sqrt{3}$ lattice site, but a little bit shifted along the $\sqrt{3}\times\sqrt{3}$ direction [Figs. 4(c) and 4(d)]. This agrees well with our STM image of an isolated cluster, as shown in Figs. 4(e) and 4(f). Moreover, our calculation shows that it is even more favorable if the clusters form a 2×2 arrangement covering the Si(111) surface. Such a process will gain energy of -0.5 eV for each cluster. This agrees again perfectly with our experimental finding of local

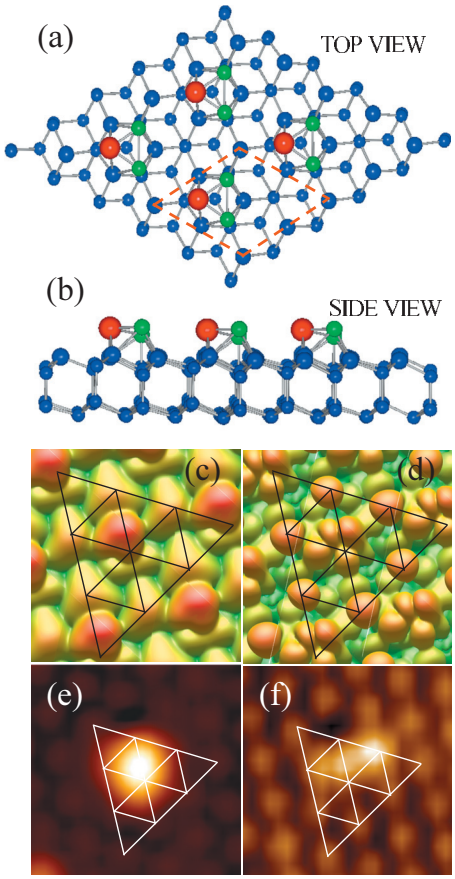

FIG. 4. (a) Top view and (b) side view of the most stable structure model of the $SiAl_2$ cluster. A unit cell of the cluster 2×2 pattern is marked by the red dotted line. Red balls are Si adatoms, green balls are Al atoms, and blue balls are substrate Si atoms. [(c) and (d)] Simulated STM images of an isolated cluster in filled state and empty states, respectively. [(e) and (f)] Filled and empty state STM images of an isolated cluster, taken at sample bias of 2.0 and -2.0 V, respectively. To clearly show the relative position of the cluster, the $\sqrt{3}\times\sqrt{3}$ lattice is outlined by grid lines in (c)–(f).

2×2 patterns formed by the clusters. The calculation also shows that the cluster is semiconducting, agreeing with our dI/dV result that shows a bandgap.

For one $SiAl_2$ cluster, to absorb extra Al atoms is not favorable. But for a congregation of clusters, extra Al atoms will cause the Al atoms to percolate among the isolated clusters due to the strong interaction between Al atoms. Thus, all Al atoms prefer to form Al-1×1 island and expel out the Si atoms. As we see from the above discussions, the formation energies of all the structures are positive, which means cost energy. For an Al island, the formation energy for each Al is -0.1 eV, which is negative and means gain energy. That is why the Al-1×1 island is the last structure while the deposition goes on.

V. CONCLUSIONS

Combining the above experimental and theoretical results, the growth mechanism of Al-1×1 film on the $\sqrt{3}\times\sqrt{3}$-Al surface can be understood. The Si adatom is the key player that continuously captures and releases Al atoms to mediate the growth of the Al-1×1 film. We should note that

the growth of monolayer Al-1×1 film is accompanied by spontaneous destroying of the underlying $\sqrt{3}\times\sqrt{3}$-Al structure and incorporation of the $\sqrt{3}\times\sqrt{3}$-Al adatoms into the growing film. The initial Al–Si bond is quite strong, while after the formation of the monolayer Al-1×1 film the Al–Si bond at the interface becomes very weak.[16] Therefore, although the final Al-1×1 structure is energetically favorable, a high energy barrier must be overcome in order to break the interface Si–Al bonds. The existence of Si adatoms provides a two-step process to achieve the final Al-1×1 structure, which is quite similar to a catalytic reaction. If there were no Si adatoms on the $\sqrt{3}\times\sqrt{3}$-Al surface, the high interface energy would result in low nucleation density of Al islands, and the usual 3D growth mode may follow. Therefore, the catalytic role play by Si adatoms is the key to achieve a 2D growth of 1 ML Al film.

In a usual epitaxial film growth process, the interface structure is not affected by the growing film. The growth is determined by the kinetics of incoming atoms on the surface, e.g., diffusion, nucleation, and islanding. We present in this paper a system where part of the substrate is being destroyed and incorporated into a growing film. A 2D growth mechanism was revealed, where the Si adatoms act as catalyst to mediate the phase transition. Such a mechanism has not been observed before, and it would provide a possibility of tailoring the growth and structure of ultrathin films by using internal dopants or defects.

ACKNOWLEDGMENTS

This work was supported by the National Natural Science Foundation of China (Grant Nos. 10874210 and 60621091), CAS, and MOST of China (Grant No. 2007CB936800).

[1] F. Rosei, J. Phys.: Condens. Matter **16**, S1373 (2004).
[2] J. V. Barth, G. Costantini, and K. Kern, Nature (London) **437**, 671 (2005).
[3] F. K. Schulte, Surf. Sci. **55**, 427 (1976).
[4] Z. Zhang, Q. Niu, and C. K. Shih, Phys. Rev. Lett. **80**, 5381 (1998).
[5] J. J. Paggel, T. Miller, and T. C. Chiang, Science **283**, 1709 (1999).
[6] T. C. Chiang, Surf. Sci. Rep. **39**, 181 (2000) and references therein.
[7] C. A. Jeffrey, E. H. Conrad, R. Feng, M. Hupalo, C. Kim, P. J. Ryan, P. F. Miceli, and M. C. Tringides, Phys. Rev. Lett. **96**, 106105 (2006).
[8] M. Jałochowski, E. Bauer, H. Knoppe, and G. Lilienkamp, Phys. Rev. B **45**, 13607 (1992).
[9] A. R. Smith, K. J. Chao, Q. Niu, and C. K. Shih, Science **273**, 226 (1996).
[10] W. B. Su, S. H. Chang, W. B. Jian, C. S. Chang, L. J. Chen, and T. T. Tsong, Phys. Rev. Lett. **86**, 5116 (2001).
[11] G. Meyer and K. H. Rieder, Appl. Phys. Lett. **64**, 3560 (1994).
[12] K. Budde, E. Abram, V. Yeh, and M. C. Tringides, Phys. Rev. B **61**, R10602 (2000).
[13] P. Czoschke, H. Hong, L. Basile, and T. C. Chiang, Phys. Rev. Lett. **91**, 226801 (2003).
[14] T. Nagao, J. T. Sadowski, M. Saito, S. Yaginuma, Y. Fujikawa, T. Kogure, T. Ohno, Y. Hasegawa, S. Hasegawa, and T. Sakurai, Phys. Rev. Lett. **93**, 105501 (2004).
[15] H. Liu, Y. F. Zhang, D. Y. Wang, M. H. Pan, J. F. Jia, and Q. K. Xue, Surf. Sci. **571**, 5 (2004).
[16] Y. Jiang, Y. H. Kim, S. B. Zhang, P. Ebert, S. Y. Yang, Z. Tang, K. H. Wu, and E. G. Wang, Appl. Phys. Lett. **91**, 181902 (2007).
[17] R. J. Hamers and J. E. Demuth, Phys. Rev. Lett. **60**, 2527 (1988).
[18] S. Landrock, Y. Jiang, K. H. Wu, E. G. Wang, K. Urban, and Ph. Ebert, Appl. Phys. Lett. **95**, 072107 (2009).
[19] M. Horn-von Hoegen and H. Pietsch, Surf. Sci. **321**, L129 (1994).
[20] Y. O. Ahn and M. Seidl, J. Appl. Phys. **77**, 5558 (1995).
[21] G. Kresse and J. Hafner, Phys. Rev. B **47**, 558 (1993); **49**, 14251 (1994).
[22] G. Kresse and D. Joubert, Phys. Rev. B **59**, 1758 (1999).